

# Mathematical Modelling of Powder Coating Polymer Extrusion in Self-Wiping Co-Rotating Twin-Screw Extruder

*Kennedy O. Amedu*

**Abstract** – The objective of this research paper is to present a unified approach for modelling and quantifying the flow, geometrical and process parameters in the local zones of the self-wiping co-rotating twin-screw extruder operated without a die as applied in the production of powder coatings in order to aid optimisation of the process. To achieve this, the flow dynamics is modelled by analysis of the velocity profile in the forward and reverse screw elements that are prevalent, from which the local drag and pressure flow rate, degree of fill in the screw channel and residence time can be determined. A new modelling approach for the flow profile in kneading disc elements is proposed. The Newtonian and non-Newtonian flow cases were considered. A model for calculating the non-Newtonian viscosity was also proposed. With these strategies proposed, it is seen that it is possible to quantify the local geometrical and flow parameters, which influence processing of powder coatings in the self-wiping co-rotating twin-screw extruder without recourse to experimental data.

Index– Drag flow rate, pressure flow rate, degree of fill, mean residence time, mean time delay, feed rate, screw speed.

## 1. Introduction

The self-wiping co-rotating twin-screw extruder is versatile equipment widely employed in the powder coatings, pharmaceutical and food industries whether for mixing or compounding purposes or just for melting. The screw configuration is usually modular with different types of screw elements in the local zones of the extruder (e.g. helical screw and kneading elements) making up the configuration.

The production of powder coatings using self-wiping co-rotating twin screw extruder, usually operated without a die, involves the melt-mixing of a premix consisting of the base polymer; usually thermosetting resins such as epoxy, polyester acrylic or polyurethane, with its constituents such as pigments, additives and fillers to give the desired product and to suit customer requirement. The primary particle size of the solid fillers and pigments is usually small enough for further breakdown during melt mixing in the extruder to be unnecessary [29]. In addition, the chemical reactivity of the thermosetting resins often imposes limitations in terms of temperature and residence time during the mixing process [29], [30].

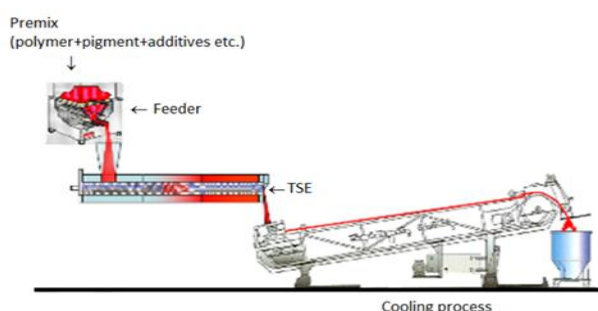


Figure 1 – Stages in the Production of Powder Coatings in Twin Screw Extruder (TSE) [31]

An in-depth understanding of the processing behaviour of powder coating premix with variations in screw speed and feed rate enables process optimisation of a range of formulations using the same extruder screw configuration, hence the need for understanding the flow dynamics in the extruder. The output from the extruder will also be greatly influenced by the bulk density of the formulations as low bulk density fillers and pigments can lead to an output limited by intake where difficulty is encountered in conveying the premix away from the feed zone to the mixing zone consisting of kneading elements [29].

Currently, optimisation of the extrusion process during powder coating production is still based on empirical approach where experimental investigation is carried out and data fitting is done to derive a suitable model. Apart from the cost and time constraint involved in this approach, there is also hindrance in the flexibility of determining the performance of the extrusion process for other processing conditions for instance when different materials are to be used or input conditions are to be varied on the same extruder configuration as well as on other extruder configuration. There are currently no detailed models from first principles which shows how the behaviour and connection of the local zones within a specific screw configuration can be analysed to enable direct quantification and optimisation of process parameters or input conditions (e.g. screw speed and feed rate) without recourse to experimental data fitting, particularly for the case of a self-wiping co-rotating twin screw extruder without a die which is prevalent in powder coating production. All the models currently

available are based on extruders with a die. Also, no detailed theoretical models exist for the analyses of flow in the partially or partly full kneading disc zones such as the forward kneading disc mostly used in powder coating production.

It has been established from past research that polymer processing in the extruder is influenced by factors such as the flow dynamics, geometrical parameters of the local zones, the operating conditions (feed rate and screw speed) as well as the material properties of the polymer (density and viscosity) [9], [11], [12]. Research has also reported that the flow dynamics is greatly controlled by the local geometrical configuration [9; 11]. For example, the stagger angle of the kneading disc used for melt mixing will dictate the degree of fill as well as the pressure flow profile. Kneading discs staggered in the forward or reverse direction will behave like a forward or reverse screw element respectively.

The geometry of the self-wiping co-rotating twin screw extruder was studied in detail by Booy in [22] who stated that the self-wiping co-rotating twin screw extruder behaves much like a single screw extruder. It was shown how the screw diameter, centerline distance, pitch and number of tips influence design, net volumes and surface areas. Kneading blocks were approximated by a screw of "equivalent pitch" in the work by Potent et al. [12]. Similar work was also carried out by Zagal et al. [11] in which the equivalent pitch, width and height of the channel of the kneading disk were determined.

In the modelling of the flow dynamics, Tadmor et al. [21] elaborated that the mathematical model of isothermal flow of a Newtonian fluid in shallow-screw channels results in a simple design equation, giving enormous understanding of the flow mechanism that is very useful for first order calculations. This model represents the standard classic pumping model for single screw extrusion. Similar work was also done by Booy [24], Meijer and Elemans [10] in which a mathematical model of isothermal flow of viscous liquids in co-rotating twin-screw extruder was developed. Kneading blocks were approximated by a screw of "equivalent pitch" in the work by Potent et al. [12], making allowance for the leakage flow across the flights from one channel to the adjacent channel. A complex systematic design suitable only for implementation via software; for the determination of the filling level profiles, the pressure profiles, the melting profiles, the residence time distributions, the temperature profiles, the shear stress profiles, and the power consumption in modular tightly intermeshing co-rotating twin screw extruders was presented

Vergnes et al. [5] proposed a simple global computational flow model for self-wiping co-rotating

twin-screw extruders considering the local zones. The flow in the screw zone was modelled using cylindrical coordinates in which the channel section is considered perpendicular to the screw flights, with special interest on flow in the peripheral  $\theta$ -direction. No attempt was made to model the flow in the intermeshing zone between the kneading disc pair.

The goal of this research work is to present a detailed modelling from first principles of powder coating extrusion in a co-rotating twin-screw extruder operated without a die. A unified logical approach for modelling, quantifying and analyzing the flow profile and geometrical parameters in the local zones of the extruder for the forward and reverse kneading discs, showing how the velocity profile evolves with the local geometrical parameters and the subsequent connectivity among the local zones to aid understanding and optimization of processing in the extruder equipment is presented. Special attention is given to the forward kneading disc elements showing how the degree of filling in the local zones can be modelled since much attention has been particularly given to fully filled reverse kneading elements in past research. Newtonian as well as Non-Newtonian flow modelling was done. A new model for analyzing the non-Newtonian viscosity behavior was proposed. Analysis of the flow in the channels of the kneading disc was carried out and a new modelling approach was proposed.

## 2. MATERIALS AND METHODS

### QUANTIFYING THE FLOW AND GEOMETRICAL PARAMETERS

Processing with the self-wiping co-rotating twin screw extruder whether for mixing or just for melting purpose, is usually influenced by the flow dynamics and the screw configuration available in the local zones. Thus for the purpose of understanding and optimization, it is necessary to quantify these parameters. The flow dynamics will be influenced by the screw geometry as well as the rheological parameters such as the viscosity of the polymer material. The screw elements such as the kneading disc can either be forward (e.g. 30 and 60-degree forward kneading disc) or reverse conveying (e.g. 30 and 60-degree reverse kneading disc). Also based on the rheology, polymer materials can either be Newtonian or non-Newtonian. The nature of the flow profile will be treated in this section. The modelling will be limited to the isothermal case.

### 2.1 Newtonian Flow in Forward Conveying Elements:

For the isothermal incompressible Newtonian flow, a fluid particle starting at the feed zone will advance in the down channel direction ( $z$  axis) in the screw channel.

Thus the volumetric flow rate  $Q_v$  is obtained by integrating the z-component of the fluid velocity vector over the cross-section of the channel perpendicular to the z-axis. Mathematically, this is given as:

$$Q_v = \int_0^h \int_0^w v_z dx dy \quad (1)$$

The continuity equation of the rectangular coordinate in the z-axis or the z component of the momentum equation for steady isothermal flow of an incompressible Newtonian fluid [21; 23], can be reduced to:

$$\frac{1}{\mu} \left( \frac{\partial P}{\partial z} \right) = \frac{d^2 v_z}{dy^2} \quad (2)$$

With boundary conditions given as:

$$v_z(0) = 0 \quad v_z(h) = V_z \quad (3)$$

Thus the solution to equation 2 above satisfying the boundary conditions can be written as:

$$v_z = y \left( \frac{V_z}{h} \right) - \frac{y(h-y)}{2\mu} \left( \frac{\partial P}{\partial z} \right) \quad (4)$$

The volumetric flow rate from the simplified flow theory reduces to;

$$Q_v = w \int_0^h v_z dy \quad (5)$$

The volumetric flow rate after introducing equation (4) into equation (5) and integrating gives;

$$Q_v = \frac{V_z w h}{2} F_d + \frac{w h^3}{12\mu} \left( -\frac{\partial P}{\partial z} \right) F_p \quad (6)$$

Where the first term is the drag flow rate and the second term is the pressure flow rate. This can be written as;

$$Q_v = Q_d - Q_p \quad (7)$$

Where;

$$Q_d = \frac{V_z w h}{2} F_d \quad (8)$$

$$Q_p = \frac{w h^3}{12\mu} \left( \frac{\partial P}{\partial z} \right) F_p \quad (9)$$

Where  $Q_v$  is the volumetric flow rate from the hopper,  $Q_d$  is the drag flow rate,  $Q_p$  is the pressure flow rate,  $F_d$  and  $F_p$  are shape factors for the drag and pressure flow respectively,  $V_z$  is the maximum down channel velocity,  $w$  and  $h$  are the width and height of the channel respectively,  $\mu$  is the viscosity of the polymer material and  $\frac{\partial P}{\partial z}$  is the down channel pressure gradient. The pressure flow, which can occur as a result of local filling particularly in the kneading disc channel, is negative, signifying positive pressure gradient or pressure rise in the direction of flow [21]. There is no backflow resulting in back pressure since there is no die.

If we divide equation (7) by  $Q_d$ , it becomes;

$$\frac{Q_v}{Q_d} = 1 - \frac{Q_p}{Q_d} \quad (10)$$

If we make  $a = \frac{y}{h}$  and  $\beta = \frac{Q_p}{Q_d}$ , then;

$$\frac{Q_v}{Q_d} = 1 - \beta \quad (11)$$

Where  $\beta$  can be written as;

$$\beta = \frac{Q_p}{Q_d} = \frac{\frac{w h^3}{12\mu} \left( \frac{\partial P}{\partial z} \right)}{\frac{V_z w h}{2}} = \frac{h^2}{6\mu V_z} \frac{\partial P}{\partial z} \quad (12)$$

Bringing  $a$  and  $\beta$  into equation (4) above, the velocity profile in the down channel direction can then be written as;

$$\frac{v_z}{V_z} = a(1 - 3\beta + 3a\beta) \quad (13)$$

Equation (13) above describes the velocity profile in the forward conveying screw elements. A plot of  $a$  against  $\frac{v_z}{V_z}$  at various  $\beta$  values for the forward conveying elements such as forward screw and kneading disc can be done to determine the variation and shape of the velocity profile in the down channel direction. This is shown in figure 2 below.

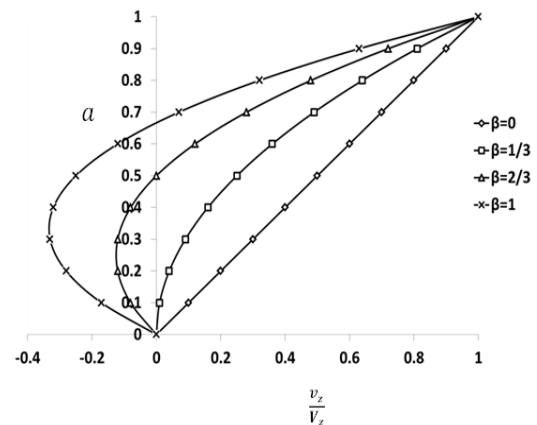


Figure 2 – Velocity profiles in forward conveying screw elements.

## 2.2 Newtonian Flow in the Reverse Conveying Elements:

For the case of the reverse screw elements, the reverse is the case in comparison to forward screw elements. Thus using the same approach for the forward conveying elements, the sign in the flow equation is changed or becomes the opposite [5], [12], [26]. Chandrasekaran and Karwe [26] carried out an experimental investigation of the velocity profile in both the forward and reverse kneading disc elements which clearly showed this assumption to be true. Thus, changing the sign of the down channel velocity in equations (4) and (7) above give the following;

$$v_z = \frac{y(h-y)}{2\mu} \left( \frac{\partial P}{\partial z} \right) - y \left( \frac{V_z}{h} \right) \quad (14)$$

$$Q_v = Q_p - Q_d \quad (15)$$

$$\frac{Q_v}{Q_d} = \frac{Q_p}{Q_d} - 1 \quad (16)$$

$$\frac{Q_v}{Q_d} = \beta - 1 \quad (17)$$

As done earlier, putting  $a$  and  $\beta$  in equation 14 results to;

$$\frac{v_z}{V_z} = a(3\beta - 3a\beta - 1) \quad (18)$$

Since the flow in the reverse kneading disc is the opposite of the forward kneading disc case, it can be assumed that the pressure flow  $Q_p$  is positive, signifying negative pressure gradient and a drop in pressure in the direction of flow. Backflow in this case occurs as a result of the reverse drag flow.

A plot of  $a$  against  $\frac{v_z}{V_z}$  at various  $\beta$  values for the reverse conveying kneading disc elements can be done to determine the variation and shape of the velocity profile in the down channel direction shown in figure 3 below.

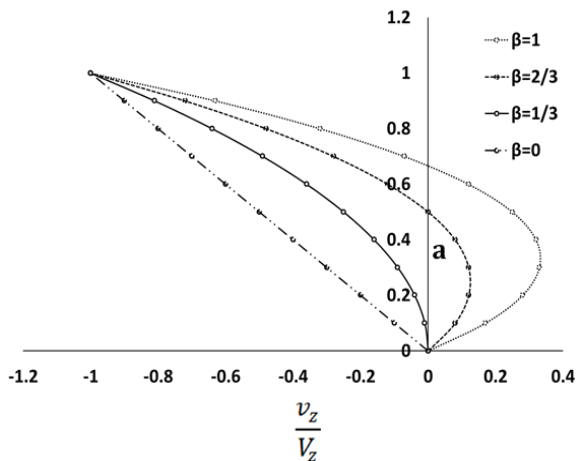


Figure 3 – Velocity profiles in reverse conveying screw elements.

The  $\beta$  value is a flow characteristic property which defines the behavior of each zone based on the geometrical configuration. Thus, the local zones will be analyzed individually to understand its behavior and how important local parameters can be quantified based on the velocity flow profile.

### 2.3 Solid Conveying Zone

The solid conveying or intake zone usually consists of helical screws with the sole function of conveying the polymer material away to the kneading disc zones in the solid state. As such, the barrel segment of the zone is usually kept at room temperature.

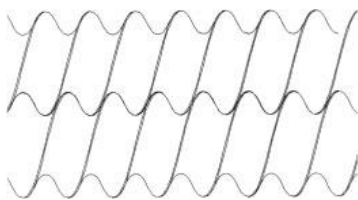


Figure 4 – Self-wiping forward helical screws

The polymer material in this zone is conveyed without any pressure development as a result of the partial filling in the zone. The boundary conditions for the flow are given in figure 5 below.

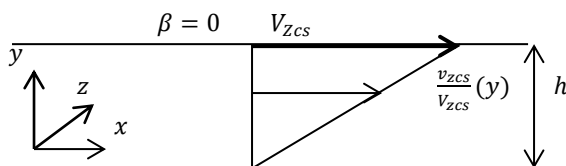


Figure 5 – Flow profile in the solid conveying zone.

The maximum velocity occurs at the surface of the rotating screw and the velocity profile is linear since there is no pressure development [18]. The exact solution of the velocity is given as;

$$v_{zcs}(y) = V_{zcs} \left( \frac{y}{h} \right) \quad (19)$$

If the helical screw with diameter  $D_s$  and a pitch angle of  $\theta_{cs}$  is rotating with speed  $N$ , the maximum velocity in the direction of flow is given as;

$$V_{zcs} = \pi D_s N \cos \theta_{cs} \quad (20)$$

The maximum drag flow rate can be given as;

$$Q_{DCS} = m \pi D_s N \cos \theta_{cs} w_{cs} h_{cs} f_{dcs} \quad (21)$$

Since there is no pressure flow ( $Q_p = 0$ ), the flow profile is linear, the mean velocity will be thus half of the maximum velocity (18). The mean flow rate is given as;

$$Q_{vcs} = Q_{dcs} \quad (22)$$

In practical operation,  $Q_{vcs} \neq Q_{dcs}$  [21], hence the degree of fill is determined from the ratio between  $Q_{vcs}$  and  $Q_{dcs}$ .

The mean drag flow rate is thus given as:

$$Q_{dcs} = \frac{m}{2} \pi D_s N \cos \theta_{cs} w_{cs} h_{cs} f_{dcs} \quad (23)$$

Where;

$$m = 2n_i - 1 \quad (24)$$

$$\theta_{cs} = \tan^{-1} \frac{p_{cs}}{\pi D_s} \quad (25)$$

$$w_{cs} = p_{cs} \cos \theta_{cs}$$

$$h_{cs} = R_b (1 + \cos \theta_{cs}) - \sqrt{(C_l^2 - R_b^2 \sin^2 \theta_{cs})} \quad (26)$$

Where  $m$  is the number of parallel channels,  $w_{cs}$  and  $h_{cs}$  are the width and height of the channel respectively,  $n_i$  is the number of screw tips,  $p_{cs}$  is the screw pitch in the solid conveying zone,  $R_b$  is the barrel radius,  $C_l$  is the centre line distance and  $f_{dcs}$ , the drag flow shape factor. The drag flow shape factor  $f_d$  is a correction factor which accounts for the curvature of the channel not taken into account in the rectangular channel. The shape factor is usually determined from the analytical solution of a two-dimensional stress balance [21] given as;

$$f_d = \frac{16w}{\pi^3 h} \sum_{i=1,3,5}^{\infty} \frac{1}{i^3} \tanh \left( \frac{i\pi h}{2w} \right) \quad (27)$$

For practical purposes ( $h/w < 0.6$ ), the correction factor can be expressed (in this case for the solid conveying helical screw zone) as;

$$f_{dcs} = 1 - 0.57 \frac{h_{cs}}{w_{cs}} \quad (28)$$

The mean residence time in the zone is given as:

$$\bar{t}_{cs} = \frac{V_{cs}}{Q_{vcs}} \quad (29)$$

$$Q_{vcs} = \frac{Q}{\rho_b} \quad (30)$$

$$V_{cs} = A_f L_{cs} \quad (31)$$

$$A_f = A_b - A_s \quad (32)$$

$$A_b = 2(\pi - \psi) R_b^2 + C_l R_b \sin \psi \quad (33)$$

$$A_s = n_i (\psi C_l^2 - C_l R_b \sin \psi) = \frac{1}{2} n_i \propto [R_s^2 - (C_l - R_s)^2] \quad (34)$$

Where  $\bar{t}_{cs}$  is the mean residence time,  $V_{cs}$  is the free volume,  $Q_{vcs}$  is the volumetric flow rate from the hopper,  $\rho_b$  is the bulk density of the polymer material,  $A_f$  is the free area,  $A_b$  is the barrel area,  $A_s$  is the screw

area,  $\psi$  is the angle bounding the interpenetration region and  $L_{cs}$  is the length in the solid conveying zone respectively. If  $f$  is the degree of fill, then the degree of fill in the solid conveying zone  $f_{cs}$  is given as:

$$f_{cs} = \frac{Q_{vcs}}{Q_{dcs}} \quad (35)$$

The mean time delay can be determined from the unfilled portion of the screw once the degree of fill has been calculated [3, 27]. Let  $t_{mcs}$  be the effective mean residence time of the polymer material in the zone. Thus:

$$t_{mcs} = f_{cs} \bar{t}_{cs} \quad (36)$$

Where;

$$\bar{t}_{cs} = t_{mcs} + t_{dcs} \quad (37)$$

Thus;

$$t_{dcs} = t_{cs} - f_{cs} \bar{t}_{cs} \quad (38)$$

$$t_{dcs} = (1 - f_{cs}) \bar{t}_{cs} \quad (39)$$

The modeling approach can also be applied in the melt conveying zones and is described below.

## 2.4 Melt Conveying Zone

The forward kneading discs such as those with 30 and 60-degree stagger angles are forward conveying elements which behave in similar fashion to right handed screw element. As such, an equivalent pitch and pitch angle can be calculated for the kneading disc [11], [12], [21], [24]. Experimental investigation has also shown that the stagger angle will influence the degree of fill with 60-degree stagger angle having a higher degree of fill (15) than the 30-degree stagger angle kneading disc. A good degree of fill is necessary for pressure development to occur. Thus it could be assumed that the kneading disc with a 60-degree forward stagger will have higher pressure development, so long as there is no backflow to cause pressure drop. The flow profile in the kneading disc zone is complex and strongly controlled by the geometry. As stated by Booy [22], an indepth knowledge of the geometry of twin screw extruder is essential for analyzing fluid flow profile. A number of channels are open through which flow can occur as shown in figure 6 below.

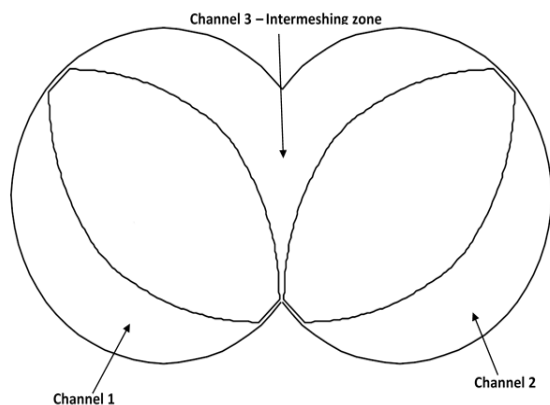


Figure 6 – Flow regions in a Kneading disc pair.

Dr. Kennedy O. Amedu is currently the CEO of OaKeen Nig. Ltd, a Research and Development Company situated in Lagos, Nigeria  
Email: kelojes39@gmail.com.

Generally, the number of channels in the kneading disc zone can be calculated based on the groove model [24].

$$m = m_c + m_f \quad (40)$$

$$m_c = 2n_i - 1 \quad (41)$$

$$m_f = \frac{\alpha n_i}{\pi} \quad (42)$$

Where  $m_c$  is the number of channels representing channels 1, 2 and 3 while  $m_f$  is the channels due to the gap between the flight and the barrel surface and  $\alpha$  is the flight tip angle. Channel 3 above represents the intermeshing zone. There is usually leakage flow in the gap between the flight of the kneading disc and the barrel. Some authors have stated that the leakage flow is negligible [24], while some have stated that substantial flow occur in these channels [10]. It could be argued or assumed that some of this leakage flow rejoins the intermeshing channel zone 3 and the other channels 1 and 2 due to pressure development within the gap or perhaps due to the rotation of the kneading discs wiping the material off the surface of the barrel, thereby making it basically three main channels in the zone as determined using equation 41 above. As given by past authors [21; 24], the flow in the kneading disc represented by  $m_c$  number of channels can be given as;

$$Q_{vm} = m_c(Q_{dkd} - Q_{pdkd}) \quad (43)$$

Where;

$$Q_{dkd} = \frac{1}{2} \pi D_s N \cos \theta_{kd} \sin \theta_{kd} w_{kd} h_{kd} f_{dkd} \quad (44)$$

$$Q_{pdkd} = \frac{w_{kd} h_{kd}^3}{12\mu} \left( \frac{dp}{dz} \right) F_{pdkd} \quad (45)$$

For the forward kneading disc, an equivalent pitch angle  $\theta_{kd}$ , channel width  $w_{kd}$ , channel height  $h_{kd}$  and shape factor  $f_{dkd}$  can be determined [11; 12] and are given as;

$$\theta_{kd} = \tan^{-1} \left( \frac{e_{kd}}{\alpha_{kd} R_s} \right) \quad (46)$$

$$w_{kd} = \frac{p_{kd} \cos \theta_{kd}}{m} - e_{kd} \quad (47)$$

$$p_{kd} = \frac{2\pi e_{kd}}{\alpha_{kd}} \quad (48)$$

$$h_{kd} = R_b \left\{ 1 + \cos \left( \frac{\alpha_{kd}}{2} \right) \right\} - \sqrt{(C_l^2 - R_b^2 \sin^2 \left( \frac{\alpha_{kd}}{2} \right))} \quad (49)$$

$$f_{dkd} = \frac{16w_{kd}}{\pi^3 h_{kd}} \sum_{i=1,3,5}^{\infty} \frac{1}{i^3} \tanh \left( \frac{i\pi h_{kd}}{2w_{kd}} \right) \quad (50)$$

Where  $\theta_{kd}$  is the equivalent pitch angle and  $p_{kd}$  is the equivalent pitch,  $e_{kd}$  is the thickness of the kneading disc,  $\alpha_{kd}$  is the stagger angle for the forward kneading disc,  $R_b$  is the radius of the barrel and  $f_{dkd}$  is the drag flow shape factor in kneading disc zone. The shape factor is controlled by the ratio between the depth and width of the channel  $h/w$ . A graphical guide for estimating the drag flow (as well as the pressure flow) shape factor once the  $h/w$  ratio is known was given by Tadmor and Gogos [21] and is shown in figure 7 below.

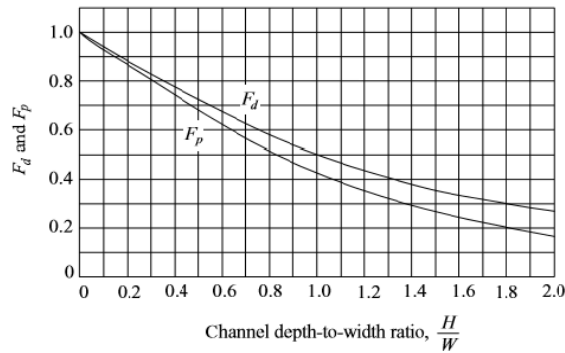


Figure 7 - Shape factors for drag and pressure flow [21].

Taking a critical look at figure 6 above, it can be seen that channel 3 cannot be same area with channels 1 and 2, suggesting the possibility of an over-estimation. Another way the modelling can be approached is by taking the intermeshing region to be two complete channels like channels 1 and 2 and subtracting the area of the cut off portion of the barrel which makes it an 8-shape from the total area. This implies that there will be four channels minus the cut off area. This is illustrated below;

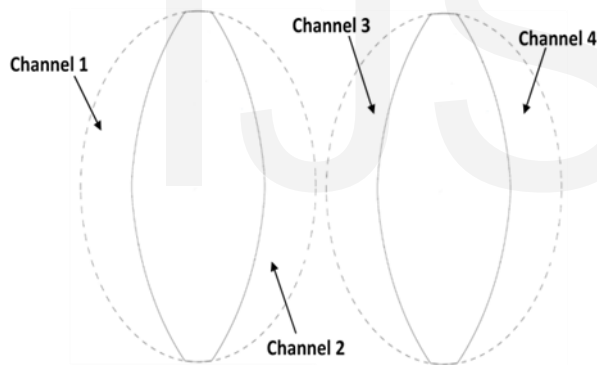


Figure 8 – Complete channels in a pair of kneading disc

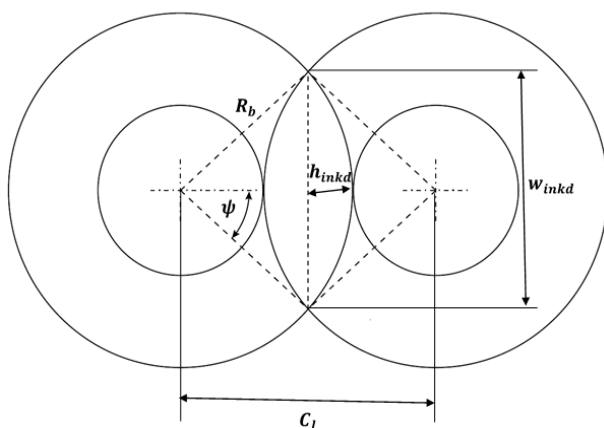


Figure 9 – Geometrical parameters of the kneading disc intermeshing zone (illustrating the cut-off area).

Dr. Kennedy O. Amedu is currently the CEO of OaKeen Nig. Ltd, a Research and Development Company situated in Lagos, Nigeria  
Email: kelojes39@gmail.com.

The resultant flow can be calculated thus;

$$Q_{vm} = 4(Q_{dckd} - Q_{pckd}) - 2(Q_{dinkd} - Q_{pinkd}) \quad (51)$$

$$Q_{dinkd} = \frac{1}{2} \pi D_s N \cos \theta_{kd} \sin \theta_{kd} w_{inkd} h_{inkd} f_{dinkd} \quad (52)$$

$$Q_{pinkd} = \frac{w_{inkd} h_{inkd}^3}{12\mu} \left( \frac{dP}{dz} \right) F_{pinkd} \quad (53)$$

$$w_{inkd} = 2 \sqrt{R_b^2 - \left( \frac{c_l}{2} \right)^2} \quad (54)$$

$$h_{inkd} = R_b - \sqrt{R_b^2 - \left( \frac{w_{inkd}}{2} \right)^2} \quad (55)$$

It can also be seen that in the models presented by Booy [24], the clearance between the kneading disc flight tip and barrel through which leakage due to pressure flow can occur has been neglected. There will be four flight tip channels in the kneading disc as seen in figure 10, as such, the pressure flow equation will be multiplied by four and the equivalent pitch angle for the kneading disc replaced with the flight tip angle. This can be approximated as follows;

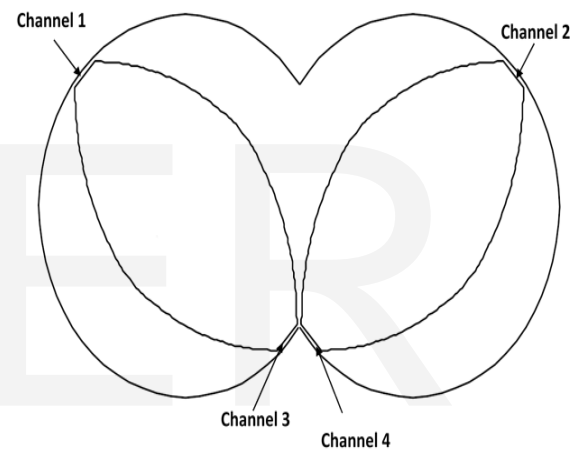


Figure 10 – Channels between the kneading disc flight tip and barrel.

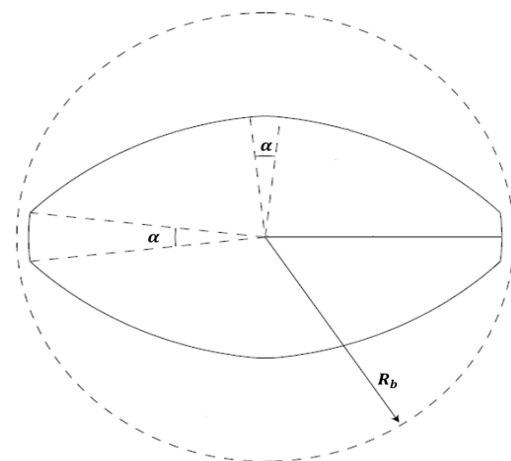


Figure 11 – Kneading disc showing the flight tip angle  $\alpha$ .

$$Q_{Lkd} = \frac{w_{Lkd} h_{Lkd}^3}{3\mu} \left( \frac{dP}{dz} \right) F_{pLkd} \quad (56)$$

$$w_{Lkd} = 2R_b \sin \left( \frac{\alpha_{kd}}{2} \right) \quad (57)$$



$$h_{Lkd} = R_b - \sqrt{R_b^2 - \left(\frac{w_{fkd}}{2}\right)^2} \quad (58)$$

$$\alpha_{kd} = \frac{\pi}{n} - 2\psi_{kd} \quad (59)$$

Thus with the inclusion of the leakage flow, the total flow in the kneading disc can then be given as;

$$Q_{vm} = 4(Q_{dckd} - Q_{pckd}) - 2(Q_{dinkd} - Q_{pinkd}) - Q_{Lkd} \quad (60)$$

Equation 60 can be rewritten thus;

$$Q_{vm} = Q_{dkd} - Q_{pkd} \quad (61)$$

Where;

$$Q_{dkd} = 2(2Q_{dckd} - Q_{dinkd}) \quad (62)$$

$$Q_{pkd} = 2(2Q_{pckd} - Q_{pinkd}) + Q_{Lkd} \quad (63)$$

## 2.5 Flow Profile in the Forward Kneading Disc

As stated earlier, the forward kneading disc behaves more like the right handed screw element in which material is conveyed in the down channel direction without any backflow in the axial direction [21]. The conveying capability is dependent on the stagger angle [11], [12], [25], thus the drag flow capacity will differ for different stagger angles. The resultant flow profile is the linear superposition of the drag and pressure flow. In this case the pressure and drag flow has velocity fields (using the analytical approach) acting in the forward direction as shown in figure 12 below:

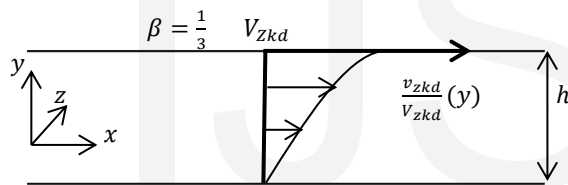


Figure 12 – Flow profile in the forward conveying kneading disc zone.

It can be observed in figure 12 above that the flow profile is a combination of drag and pressure flow. The drag flow occurs as a result of the rotation of the screws while the pressure flow results due to pressure developed as a result of the smearing action between the barrel and kneading disc resulting from the local filling of the zone with the polymer material.

For the case of the forward kneading disc, pressure increases in the direction of flow i.e. the pressure gradient is positive and thus, the pressure flow term  $Q_p$  is negative ( $Q_v < Q_d$ ).

From figure 12 above, it can be deduced that an approximate mean pressure flow rate for the forward kneading disc  $Q_{pkd}$  is given as;

$$Q_{pkd} = \frac{Q_{Dkd}}{3} \quad (64)$$

The mean drag flow rate in the down channel  $Q_{dkd}$  is given as:

$$Q_{dkd} = \frac{Q_{Dkd}}{2} \quad (65)$$

It can be easily deduced from equations 61, 64 and 65 that the net flow rate is given as;

Dr. Kennedy O. Amedu is currently the CEO of OaKeen Nig. Ltd, a Research and Development Company situated in Lagos, Nigeria  
Email: kelojes39@gmail.com.

$$Q_{vm} = \frac{Q_{Dkd}}{2} - \frac{Q_{Dkd}}{3} = \frac{Q_{Dkd}}{6} \quad (66)$$

Similarly, as analyzed for the solid conveying zone,  $Q_{vm} \neq \frac{Q_{Dkd}}{6}$  in practical operation as the extruder is run from a metered hopper, hence the degree of fill in the melt conveying forward kneading disc can then be determined from the ratio between  $Q_{vm}$  and  $\frac{Q_{Dkd}}{6}$ .

Applying a similar approach used in the solid conveying zone, the mean residence time equations are derived thus [27];

$$\bar{t}_{kd} = \frac{V_{kd}}{Q_{vm}} \quad (67)$$

$$Q_{vm} = \frac{Q}{\rho_m} \quad (68)$$

$$\bar{t}_{mkd} = f_{kd} \bar{t}_{kd} \quad (69)$$

$$\bar{t}_{kd} = \bar{t}_{mkd} + \bar{t}_{dkd} \quad (70)$$

$$f_{kd} = \frac{Q_{vm}}{Q_{Dkd}/6} \quad (71)$$

$$V_{kd} = A_f L_{kd} \quad (72)$$

$$\bar{t}_{dkd} = \bar{t}_{kd} - f_{kd} \bar{t}_{kd} \quad (73)$$

Here,  $Q_{vm}$  is the volumetric flow rate,  $\bar{t}_{kd}$ ,  $\bar{t}_{mkd}$  and  $\bar{t}_{dkd}$  are the total, effective mean residence time and the mean time delay respectively,  $V_{kd}$  is the free volume,  $f_{kd}$ ; the degree of fill and  $\rho_m$  is the melt density at the average fluid temperature of the polymer material, all in the kneading disc zone.

## 2.6 Flow Profile in the Reverse Kneading Disc

In the case of the reverse kneading disc, the two dominating flow, i.e., the drag and pressure flow change directions. The presence of back flow in this case is due to drag while the pressure flow is the forward flow as shown in figure 3 above. The degree of fill is greater than unity. The flow profile is basically the reverse of the forward kneading disc elements. Analysis of the flow profile shows that, for there to be flow advancement in the forward direction of the down channel as can be seen from figure 3, it can be assumed that  $\frac{Q_{pkd}}{Q_{dkd}}$  must be greater than 1/3 ( $\frac{Q_{pkd}}{Q_{dkd}} > 1/3$ ) but less than or equal to 2/3 ( $\frac{Q_{pkd}}{Q_{dkd}} \leq 2/3$ ) on average, since at  $\beta = 1$ , the drag and pressure flow are equal which can stall the flow and possibly not obtainable in this case of an extruder without a die.

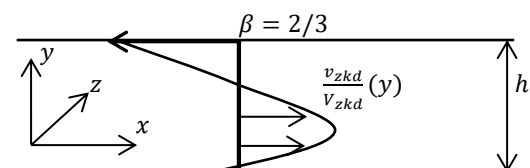


Figure 13 – Flow profile in the reverse conveying kneading disc zone.

Thus;

$$Q_{pkd} = \frac{2Q_{Dkd}}{3} \quad (74)$$

$$Q_{vm} = \frac{-Q_{Dkd}}{2} + \frac{2Q_{Dkd}}{3} = \frac{Q_{Dkd}}{6} \quad (75)$$

It will also be expected for the reverse kneading disc element to behave in the reverse way in terms of the conveying capacity. Thus the 30 and 60-degree reverse kneading disc becomes -60 and -30 degree kneading disc respectively. This implies that the -60 degree kneading disc can be assumed to have more backflow, hence less conveying capability than the -30 degree kneading disc.

$$\bar{t}_{kd} = \frac{V_{kd}}{Q_{vm}} \quad (76)$$

$$\bar{t}_{mkd} = \bar{t}_{kd}(1 + f_{kd}) \quad (77)$$

$$f_{kd} = \frac{Q_{vm}}{Q_{Dkd}/6} \quad (78)$$

Looking at equations 76 – 78, it has been assumed that degree of filling will be greater than unity because of the backflow caused by the reverse drag flow. This is shown in equation 77 with the degree of fill  $f_{kd}$  assumed to be the extra fill beyond unity similar to that of the forward conveying kneading disc.

## 2.7 The 90 degree kneading disc and the metering zone

The 90 degree kneading disc has zero conveying capacity as polymer material in this zone is usually transported away by the preceding conveying kneading discs [21]. It is assumed to be always fully filled because it is non-conveying (5; 8; 13) no matter the feed rate and screw speed as fluid material must accumulate and fill up the length of the zone before there can be transport away from the zone by the preceding forward conveying zones. Also, the metering zone which is without a die in this work, preceded by the 90 degree kneading disc zone in this investigation is fully filled Newtonian flow model has to be modified to account for the changing viscosity. There are several viscosity equations for non-Newtonian fluids such as the Power law, Carreau, Reiner-Philippoff and the Ellis model [21], to mention just a few. The Power law model is frequently used and can describe the shear-thinning behavior of polymers with good accuracy. The Power law model for isothermal non-Newtonian flow is given as;

$$\mu = K\dot{\gamma}^{n-1} \quad (81)$$

Where  $K$  and  $n$  are the consistency and flow index respectively for a specific polymer material while  $\dot{\gamma}$  is the shear rate. For shear thinning fluids,  $n < 1$ . When the flow index  $n$  is unity, the power law reduces to the Newtonian law. The shear rate  $\dot{\gamma}$  is given as;

$$\dot{\gamma} = \frac{dv_z}{dy} |_{y=h} \quad (82)$$

Equation 82 can thus be solved by differentiating the down channel velocity equation in equation 4 above.

This gives;

$$\frac{dv_z}{dy} = \frac{d}{dy} \left[ \frac{V_z}{h} - \left( \frac{y h + y^2}{2\mu} \right) \frac{dP}{dz} \right] \quad (83)$$

$$\frac{dv_z}{dy} |_{y=h} = \frac{V_z}{h} - \left( \frac{h+2h}{2\mu} \right) \frac{dP}{dz} \quad (84)$$

$$\dot{\gamma} = \frac{V_z}{h} + \frac{h}{2\mu} \frac{dP}{dz} \quad (85)$$

(basically with a shorter length than the preceding 90 degree kneading disc zone) to be able to generate the pumping pressure at the exit of the extruder [8], [13]. Aside this, the screw pitch in the metering zone is usually smaller than that of the feed zone (solid conveying zone) to enable it generate pressure. Note that if the metering zone is not preceded by a 90-degree kneading disc but by forward kneading discs for instance, then the degree of filling could be influenced by the operating conditions of screw speed and feed rate and thus the approach used for the melt conveying forward kneading disc will apply. In this case of a fully filled condition, the mean residence time is given as:

$$\bar{t}_{ff} = \frac{V_{ff}}{Q_{vm}} \quad (79)$$

$$V_{ff} = A_f L_{ff} \quad (80)$$

Where  $\bar{t}_{ff}$  is the mean residence time,  $V_{ff}$  is the volume,  $L_{ff}$  is the length of the fully filled zones and  $Q_{vm}$  is the volumetric flow rate.

Experimental investigation can be carried out for validation purposes to determine if the process variables in the model such as the mean residence time and mean time delay quantified theoretically has been properly done.

## 2.8 Non-Newtonian Flow

In the Newtonian flow model presented above, the viscosity is independent of the shear rate. Most molten polymer materials are shear thinning or pseudoplastic in nature, i.e., its viscosity decreases with increasing shear rate or shear stress. Thus the viscosity parameter in the

Rearranging equation 85 for the pressure gradient gives:

$$\frac{dP}{dz} = \left( \dot{\gamma} - \frac{V_z}{h} \right) \frac{2\mu}{h} \quad (86)$$

Also rearranging equation 4 above for the pressure gradient results in;

$$\frac{dP}{dz} = \left( \frac{V_z h}{2} F_d - Q_v \right) \frac{12\mu}{wh^3 F_p} \quad (87)$$

Equating equation 86 and 87 gives;

$$\left( \dot{\gamma} - \frac{V_z}{h} \right) \frac{2\mu}{h} = \left( \frac{V_z h}{2} F_d - Q_v \right) \frac{12\mu}{wh^3 F_p} \quad (88)$$

Neglecting the shape factors for now, equation 88 simplifies to;

$$\dot{\gamma} = \frac{2}{h} \left( 2V_z - \frac{3Q_v}{wh} \right) \quad (89)$$

Thus, equation 81 can now be rewritten as;

$$\mu = \frac{2K}{h} \left( 2V_z - \frac{3Q_v}{wh} \right)^{n-1} \quad (90)$$

Thus, the viscosity changes according to equation 90 and replaces the viscosity in equation 4 above to characterize the non-Newtonian behavior of the fluid.

## 3. RESULTS AND DISCUSSION

### Analysis of the Flow Profile:

Figure 2 above shows the velocity profile in the down channel direction for the forward conveying elements. In the  $y - z$  plane, the shear pattern is greatly dependent



on the value  $\beta$ . This is quite an important parameter to consider since transport or fluid advancement occurs mainly in the down channel direction (z-direction) as flow in the x-direction is a circulatory flow with no flow advancement. Though flow in the z-direction (down Note that velocity vectors in the down channel direction (z – plane) for the forward kneading disc has all positive values only for  $\beta \leq 1/3$  whereas for  $\beta > 1/3$ , it has both positive and negative values. This implies that the optimum filling level for there to be no backflow occurs at  $\beta = 1/3$ . Further increase in the value of  $\beta$  will result in backflow, thereby slowing down the advancement of the fluid towards the discharge port. This also indicates that at  $\beta = 1/3$ , the local forward kneading block reaches its inherent throughput, further increase which will result in backflow. This case occurs when the forward kneading block is overrun (increase in throughput or feed rate at a given screw speed is larger than the amount of fluid material the local zone can accommodate) for example by a preceding or previous zone with a higher pumping capacity. This phenomenon of the occurrence of backflow or the local kneading block exceeding its inherent throughput thus leads to pressure drop (positive and negative pressure values with a resultant reduction in net pressure rise). In this case, the local forward kneading block must now feed more per revolution than the maximum possible throughput during the pressure-free conveying [9], [12]. For the flow in the reverse conveying elements as shown in figure 3, the drag flow is in the reverse direction while the pressure flow is in the forward direction. There must be considerable increase in the pressure flow for there to be effective advancement of fluid downstream since the drag component of flow conveys the fluid in the upstream direction, making the pressure flow dominant. In a sense, the pressure flow must exceed the drag flow of the reverse kneading disc for there to be forward movement of the fluid, thus implying that forward flow occurs by pressure drop [28]. This implies that the local screw element must be fully filled beyond unity for this to occur, hence the dominance of pressure flow over drag flow in the reverse kneading disc. As such,  $\beta$  must always be greater than  $\frac{1}{3}$  ( $\beta > 1/3$ ) as can be seen in figure 3 above. The reverse kneading disc acts like a flow obstacle in similar fashion as a die which generates a drop in pressure. Thus  $\beta$  must have an average value of  $2/3$  for there to be effective flow advancement. Again for the case of  $\beta = 1$ , for which there is equal drag and pressure flow, there will be no flow advancement in the axial direction as the fluid particle simply advances and retreats in the channel. This case will not be obtainable for the extruder run without a die.

channel) is also a circulatory or rotational flow but makes a flow advancement in the axial direction equivalent to the pitch length for each turn of screw [12], [22], [24].

#### 4. CONCLUSION

Following a unified logical approach in modelling, quantifying and analyzing the flow and geometrical parameters in the local zones of a self-wiping co-rotating twin-screw extruder, gives a clearer understanding of the interrelationship among these parameters thereby aiding optimization of powder coating polymer processing in the extruder equipment. It is possible to analyze and quantify from first principles the flow and geometrical parameters and relate these to the operating conditions for a self-wiping co-rotating twin screw extruder to aid the process operator in making decisions and maximizing output from the extruder.

#### 5. REFERENCES

- [1] J. Gao, C.G. Walsh, D. Bigio, R.M. Briber and M.D. Wetzel, "Mean Residence Time Analysis for Twin Screw Extruders", *Polym Eng. Sci.*, 40, 1, pp. 227-237, 1999.
- [2] J. Gao, C.G. Walsh, D. Bigio, R.M. Briber and M.D. Wetzel, "Residence-Time Distribution Model for Twin-Screw Extruders", *AIChE J.*, 45, 12, pp. 2541-2549, 1999.
- [3] A. Poulesquen and B. Vergnes, "A Study of Residence Time Distribution in Co-Rotating Twin-Screw Extruders. Part I: Theoretical Modelling", *Polym. Eng. Sci.*, 43, 12, pp. 1841-1848, 2003.
- [4] A. Poulesquen and B. Vergnes, "A study of residence time distribution in co-rotating twin-screw extruders. Part II: Experimental Validation", *Polym. Eng. Sci.*, 43, 12, pp. 1849-1862, 2003.
- [5] B. Vergnes, G.D. Valle and L. Dellamare, "A Global Computer Software for Polymer Flows in Co-rotating Twin Screw Extruders", *Polymer Eng Sci*, 38, 11, pp. 1781-1792, 1998.
- [6] E.G. Gasner, D. Bigio, C. Marks, F. Magnus and C. Kiehl, "A New Approach to Analyzing Residence Time and Mixing in a Co-Rotating Twin Screw Extruder", *Polym. Eng. Sci.*, 39, 2, pp. 286-298, 1999.
- [7] J.P. Puaux, G. Bozga and A. Ainser, "Residence time distribution in a co-rotating twin-screw extruder", *Chem. Eng. Sci.*, 55, 9, pp. 1641-1651, 2000.
- [8] L.P.B.M. Janssen and L. Moscicki, "Design and Modelling of Self Wiping Twin Screw Food Extruders", *OL PAN*, 10, pp. 128-135, 2010.
- [9] K. Kohlgrubber, "Co-Rotating Twin Screw Extrusion – Fundamentals, Technology and Applications", Carl-Hanser, Munich, 2008.

- [10] H.E.H. Meijer and P.H.M. Elemans, "Modelling of Continuous Mixers. Part I: The Co-rotating Twin-Screw Extruder", *Polym Eng. Sci.*, 28, 5, pp. 275-290, 1988.
- [11] A. Zagal, E. Vivaldo-Lima and O. Manero, "A Mathematical Model for the Reactive Extrusion of Methyl Methacrylate in a Co-rotating Twin-Screw Extruder", *Ind. Eng. Chem. Res.*, 44, 26, pp. 9805-9817, 2005.
- [12] H. Potente, J. Ansahl and B. Klarholz, "Design of Tightly Intermeshing Co-Rotating Twin Screw Extruders", *Intern. Polym. Proc.*, IX, 1, pp. 11-25, 1994.
- [13] L.P.B.M. Janssen, P. Sutanto and F. Picchioni, "Modelling a continuous devulcanization in an extruder", *Chem. Eng. Sci.*, 61, pp. 7077-7086, 2006.
- [14] H.F. Giles, J.R. Wagner and E. M. Mount, "Extrusion: The Definitive Processing Guide and Handbook", William Andrew, New York, 2004.
- [15] D.M. Kalyon, C. Jacob and P. Yaras, "An experimental study of the degree of fill and melt densification in fully-intermeshing, co-rotating twin screw extruders", *Plastic, Rubber and Composites Processing and Applications*, 16, 3, pp. 193-200, 1991.
- [16] A. Kumar, G.M. Ganjyal, D.D. Jones and M. Hanna, "Modelling Residence Time Distribution in a Twin-Screw Extruder as a Series of Ideal Steady-State Flow Reactors", *Food Eng.*, 84, 3, pp. 441-448, 2008.
- [17] M. Erol and D.M. Kalyon, "Assessment of the Degree of Mixedness of Filled Polymers", *Intern. Polym. Proc.*, XX, 3, pp. 228-237, 2005.
- [18] J. Katz, "Introductory Fluid Mechanics", Cambridge University Press, New York, 2010.
- [19] L. Chen, Z. Pan and G. Hu, "Residence time distribution in screw extruders", *AICHE J.*, 39, 9, pp. 1455-1464, 1993.
- [20] R. McDonald, "Colour Physics for Industry", Society for Dyers and Colourists, Bradford, 1997.
- [21] Z. Tadmor and C.G. Gogos, "Principles of Polymer Processing", Second Edition, John Wiley & Sons, 2006.
- [22] M.L. Booy, "Geometry of Fully Wiped Twin-Screw Equipment", *Polym. Eng. Sci.*, 18, 12, pp. 973 - 984, 1978.
- [23] J.M. McKelvey, "Polymer Processing", John Wiley and Sons Inc., New York, 1962.
- [24] M.L. Booy, "Isothermal Flow of Viscous Liquids in Corotating Twin Screw Extruders", *Polym. Eng. Sci.*, 20, 18, pp. 1220 - 1228, 1980.
- [25] Y. Wang, "Compounding in Co-Rotating Twin-Screw Extruders", Rapra Technology Ltd., Shropshire, UK, 2000.
- [26] M. Chandrasekaran, and W. Karwe, "Measurement of Velocity Profiles in Reverse-Screw Elements of a Twin-Screw Extruder", *AICHE J.*, 43, 10, pp. 2424-2431, 1997.
- [27] A.O. Kennedy, P. Roger, and B. Krishna, "A Novel Modelling Approach to the Mixing Process in Twin Screw Extruders", *AIP Conf. Proc.*, 1593, 1, pp. 29 - 38, 2014.
- [28] M. Maskan and A. Altan, "Advances in food extrusion technology", Boca Raton: CRC Press, 2012.
- [29] M. Dillon "Twin screw extruders in the production of powder" European Powder Coatings Handbook and Directory, 1998.
- [30] J.A. Scott and J.T. Walters, "Residence Time Distribution Modelling for Co-rotating Twin Screw Extrusion of Thermoset Powder Coatings, *Trans IChem*, 73, A, pp. 27 - 33, 1995.
- [31] AkzoNobel, "Powder Coatings Twin Screw Extruder Technology".